Available online at www.sciencedirect.com

ScienceDirect

www.elsevier.com/locate/jes

JES JOURNAL OF ENVIRONMENTAL SCIENCES

www.jesc.ac.cn

Rapid field testing of mercury pollution by designed fluorescent biosensor and its cells-alginate hydrogel-based paper assay

Yanan Zheng[1], *Liudan Wei*[1], *Linwei Duan*[2], *Fangfang Yang*[3], *Guixiang Huang*[1], *Tianyi Xiao*[1], *Min Wei*[1], *Yanling Liang*[1], *Huiting Yang*[1], *Zhipeng Li*[2,*], *Dan Wang*[1,*]

[1] *College of Chemistry and Materials, Guangxi Key Laboratory of Natural Polymer Chemistry and Physics, Nanning Normal University, Nanning 530001, China*

[2] *State Key Laboratory for Conservation and Utilization of Subtropical Agro–Bioresources, Guangxi University, Nanning 530004, China*

[3] *Guangxi-ASEAN Food Inspection and Testing Center, China*

ARTICLE INFO

Article history:
Received 31 October 2020
Revised 24 December 2020
Accepted 6 January 2021

Keywords:
Mercury pollution
Fluorescent biosensor
Mercury detection
In natural setting
Cells-alginate hydrogel-based paper

ABSTRACT

With increasing industrial activities, mercury has been largely discharged into environment and caused serious environmental problems. The growing level of mercury pollution has become a huge threat to human health due to its significant biotoxicity. Therefore, the simple and fast means for on-site monitoring discharged mercury pollution are highly necessary to protect human beings from its pernicious effects in time. Herein, a "turn off" fluorescent biosensor (mCherry L199C) for sensing Hg^{2+} was successfully designed based on direct modification of the chromophore environment of fluorescent protein mCherry. For rapid screening and characterization, the designed variant of mCherry (mCherry L199C) was directly expressed on outer-membrane of *Escherichia coli* cells by cell surface display technique. The fluorescent biosensor was characterized to have favorable response to Hg^{2+} at micromole level among other metal ions and over a broad pH range. Further, the cells of the fluorescent biosensor were encapsulated in alginate hydrogel to develop the cells-alginate hydrogel-based paper. The cells-alginate hydrogel-based paper could detect mercury pollution in 5 min with simple operation process and inexpensive equipment, and it could keep fluorescence and activity stable at 4 °C for 24 hr, which would be a high-throughput screening tool in preliminarily reporting the presence of mercury pollution in natural setting.

* Corresponding authors.
E-mails: zp.li@gxu.edu.cn (Z. Li), 20170202@nnnu.edu.cn (D. Wang).

https://doi.org/10.1016/j.jes.2021.01.003
1001-0742/

Introduction

Nowadays, mercury has been extensively used in industries such as automobile manufacturing, oil refinery, electric power, battery facilities, and military wastes (Mojammal et al., 2019; Semu et al., 1986; Tchounwou et al., 2003; Wang et al., 2004). Accompanied by industrial production, large amounts of mercury have been discharged with industrial effluents into the natural environment. The discharged mercury tends to accumulate in the human body and cause serious brain damage as well as kidney problems (Bridges and Zalups, 2017; Ekinci et al., 2014; Ellingsen et al., 2000; Syversen and Kaur, 2012). In order to decrease the level of exposure of human beings to mercury, it is extremely important to develop economical and practical techniques to detect mercury contamination timely in the field. At present, there are various conventional technical means and devices for detecting mercury ions, such as atomic absorption spectrometry (AAS), atomic fluorescence spectrometry (AFS), and inductively coupled plasma atomic emission spectrometry (ICP-AES) (Gao et al., 2012; Liang et al., 2003; Nolan and Lippard, 2008; Sánchez-Rodas et al., 2010). All of which have good sensitivity and selectivity, however, there are several limitations in using of these detection methods and devices. The disadvantages, such as expensive cost of instrument and maintenance, complex pretreatment, high-quality workplace, and professional operator, which greatly restrict them to be used as field-portable devices directed toward simple and fast analysis in natural setting.

Fluorescence spectroscopy serves as a powerful tool for the detection of heavy metals. To date, a number of fluorescent probes for sensing metal ions have been largely developed, including nanoparticles, biomolecules, foldamers, small molecules, and synthetic polymers (Chen et al., 2015; Guo et al., 2015; Li et al., 2014; Zhang et al., 2016). The fluorescent proteins were also efficiently utilized in detecting heavy metals by using inherent and engineered metal binding properties (Ayyadurai et al., 2011; Hao et al., 2018; Jiang et al., 2015; Liu et al., 2013; Özyurt et al., 2019; Qin et al., 2016). In addition, due to the property of genetically encodable, the fluorescent proteins have unique advantages in tracking metal dynamics inside living cells (Newman et al., 2011; Nolan and Lippard, 2008). However, they were hardly applied to detect metal pollution in practice because of the difficulties in preparing and preserving. Therefore, it's worth trying to overcome the limitations and apply the fluorescent proteins for on-site detection of metal ions in industrial effluents.

In this study, a Hg^{2+}-responsive variant (mCherry L199C) of fluorescent protein mCherry was successfully designed by direct modification of the chromophore environment. Through introducing a cysteine in the vicinity of fluorophore, the fluorescent protein mCherry L199C will quench its fluorescence in the presence of Hg^{2+}. The designed fluorescent protein variant was systematically characterized through the cell surface display technique. By expressing on outer-membrane of *E.coli* cells, the variant mCherry L199C could recognize micromole level of Hg^{2+}, and it could detect Hg^{2+}in the presence of other metal ions as well as different pH environment. The cells-alginate hydrogel-based paper was further prepared to meet the requirements of rapid and field testing of mercury pollution. Relevant experiments showed that the developed cells-alginate hydrogel-based paper processed good stability in fluorescence and activity, which can analyze micromole level of Hg^{2+} within 5 min in a portable and robust fashion. By using the cells-alginate hydrogel-based paper, rapid field testing of mercury pollution in semi-quantitative can be realized in the absence of highly specialized facilities, laboratory workplaces, and professional operators.

1. Materials and methods

1.1. Strains, plasmids, media, and reagents

Escherichia coli (*E.coli*) DH5α strain [F^-, φ80d*lacZ*ΔM15, Δ(*lacZYA-argF*) U169, *hsd*R17 ($r^-\kappa$, $m^+\kappa$), *rec*A1, *end*A1, *deo*R, *thi*-1, *sup*E44, *gyr*A96, *rel*A1, λ^-] was used as the host cell for recombinant DNA construction. *E.coli* BL21(DE3) strain [F^-, *ompT*, *hsdS*$_B$ ($r_B^-m_B^-$), *gal* (λ*cl*857, *ind*1, *Sam*7, *nin*5, *lac*UV5-T7*gene*1), *dcm*(DE3)] was used as the host cell for expressing the biosensing systems. Plasmid pET30α, a low copy number plasmid carrying kanamycin resistance, which was used to express fusion genes of OmpA-mCherry and OmpA-mCherry L199C proteins. All *E.coli* cells were cultivated in Luria Bertani (LB) medium (1% (W/V) tryptone, 0.5% (W/V) yeast extract, and 1% (W/V) NaCl). The analytical standard solutions of different metal ions (Hg^{2+}, Cr^{3+}, Fe^{3+}, Cu^{2+}, Ni^{2+}, Zn^{2+}, Cd^{2+}, Pb^{2+}, and Ag^+) are existed in the form of nitrates in 1 mol/L or 1% nitric acid, and the metal ion Cr^{3+} is existed in the form of chloride in 1 mol/L hydrochloric acid. All the chemical reagents were purchased from Shanghai Aladdin Biochemical Technology Co. Ltd. The high purity deionized water (resistivity 18 MΩ • cm) for all experiments was produced by the Millipore water purification system. The industrial wastewater was provided by Guangxi Nanning Water Resources Bureau.

1.2. Construction and cultivation of the biosensor

In this study, the biosensing systems were constructed by using pET30α as expression vector in the following steps. The DNA fragment encoding 1 ~ 159 amino acids of OmpA protein (GenBank: CP034595.1) was fused to the N-terminal of gene encoding mCherry protein (GenBank: MK160997.1). The residues 1 ~ 159 of OmpA protein, which are the cell surface exposed area of the outer-membrane protein OmpA, had been successfully used as the surface presentation of many larger passengers (van Bloois et al., 2011). The fusion gene of OmpA-mCherry was amplified from the laboratory plasmid via primer I and primer II. The PCR product was cloned into pET30α vector between NdeI and XhoI restriction sites, and it was transformed into *E.coli* DH5α cell by chemical method. The construct *ompA-mcherry*-pET30α was confirmed by sequencing and finally transformed into *E.coli* BL21(DE3) strain for being induced expression. The gene of OmpA-mCherry L199C variant, which was also cloned into plasmid pET30α, was obtained by site-directed mutagenesis with primer III and primer IV. The oligonucleotides used in the construction of expression plasmids were listed in Appendix A Table S1. The protein

and gene sequences of mCherry protein as well as its mutant mCherry L199C were displayed in Appendix A Fig. S1. The differences of protein and gene sequences between mCherry and mCherry L199C were also indicated in Appendix A Fig. S1.

The *E.coli* BL21(DE3) cells with the aforementioned constructs transformed in were grown in LB medium containing 30 μg/mL of kanamycin, which were cultivated at 37 °C with constantly shaking at 250 r/min. The overnight bacteria cells were further cultivated in the LB medium after inoculum enlargement at a proportion of 1:100, and they were continued to grow until an optical density of OD600≈0.5 ~ 0.6 reached. Then, 0.1 mmol/L IPTG were added to the cultural medium to induce the expression of fusion proteins. After being induced for additional time, the cells with target proteins expressing were harvested by centrifugation. A schematic diagram (Appendix A Fig. S2) was provided to present the production process of the fusion protein of membrane protein OmpA with mCherry protein as well as its mutant (mCherry L199C) on the outer membrane of *E. coli* cells.

1.3. SDS-PAGE identification of the biosensor

To identify the successful expression of fusion proteins, the harvested biosensor cells were taken for analysis by SDS-PAGE according to the following procedures. The harvested biosensor cells were resuspended in 10 mmol/L PBS buffer (pH 7.4) and disintegrated by sonication. The cell membrane fraction was separated from the supernatant by centrifugation, and it was treated twice with TDSET buffer (1% Triton X-100, 0.2% sodium deoxycholate, 0.1% SDS, 10 mmol/L tetrasodium EDTA, and 10 mmol/L Tris/HCl) (Wei et al., 2014). Then, the biosensor cells, supernatant fraction, and membrane fraction were separately mixed with 5 × SDS PAGE loading buffer, and they were heated at 95 °C for 10 min before loading on to SDS-PAGE gel. Finally, the samples loaded onto SDS-PAGE gel were electrophoresed for 60 min under constant current.

1.4. Mercury detection with the biosensor

To evaluate its response towards Hg^{2+}, the cells of biosensor were harvested by centrifugation after being induced by 0.1 mmol/L IPTG for 8 hr. They were resuspended in 10 mmol/L PBS buffer (pH 7.4) with graded concentrations of Hg^{2+} (0 ~ 10 μmol/L). The fluorescence of the cell samples was measured by fluorescence spectrophotometer after the biosensor cells were incubated under dark conditions in the solutions containing Hg^{2+} for 1.5 hr at room temperature.

For the evaluation of detection selectivity towards Hg^{2+}, some other metal ions, such as Cr^{3+}, Fe^{3+}, Cu^{2+}, Ni^{2+}, Zn^{2+}, Cd^{2+}, Pb^{2+}, and Ag^{+} were respectively added into 10 mmol/L PBS buffer (pH 7.4) for replacing Hg^{2+}. Further, the mixture of Hg^{2+} and other metal ions were separately added into 10 mmol/L PBS buffer (pH 7.4) for replacing Hg^{2+}, too. Both the concentrations of Hg^{2+} and other metal ions were 10 μmol/L. The cell samples were also kept under dark conditions and incubated at room temperature for 1.5 hr before taking for fluorometric analysis.

To evaluate the pH effect on the detection of Hg^{2+}, the harvested biosensor cells were resuspended in the buffers with different pH values (pH = 4.0, 5.0, 6.0, 7.0, 8.0, 9.0, and 10.0). Then, 1 μmol/L Hg^{2+} were added into the buffers providing different pH environment. The buffers with different pH values are prepared by 10 mmol/L citrate-sodium citrate (pH = 4.0), 10 mmol/L citrate-sodium citrate (pH = 5.0), 10 mmol/L citrate-sodium citrate (pH = 6.0), 10 mmol/L Tris–HCl (pH = 7.0), 10 mmol/L Tris–HCl (pH = 8.0), 10 mmol/L Na_2CO_3–$NaHCO_3$ (pH = 9.0), and 10 mmol/L Na_2CO_3–$NaHCO_3$ (pH = 10.0). The cell samples before and after adding Hg^{2+} for 1.5 h were kept under dark conditions and taken for fluorometric analysis, too.

The fluorometric analysis was performed using Shimadzu RF-6000 fluorescence spectrophotometer with 580 nm and 613 nm for the excitation and emission wavelengths, respectively. Then, the intensity values at 613 nm were recorded to analyze. All the aforementioned cell samples were prepared by quintuplicate for fluorometric analysis.

1.5. Preparation of cells-alginate hydrogel-based paper

The alginate hydrogel was synthesized with 1% sodium alginate solution stirring at 40 °C for 4 hr. After passing through 0.4 μm filter, the 1% sodium alginate solution and biosensor cells were mixed uniformly in a volume ratio of 2:1. Then, 20 μL of prepared mixture was added to 0.1 mol/L $CaCl_2$ solution dropwise at a constant speed, and particles with an average diameter of 3.0 ± 0.4 mm were formed in the $CaCl_2$ solution container. In this way, an alginate network was formed by alginate cross-linking with divalent calcium ions through their carboxyl groups. The biosensor cells were further captured in the alginate network. The particles of cells-alginate hydrogel was further immobilized on the black paper strips by embedding in the punched holes with similar diameter. The procedures and pictures taken from different angles (Appendix A Fig. S3) were provided to display the immobilization of cells-alginate hydrogel on black paper. Then, the cells-alginate hydrogel-based paper for the detection of $Hg^{2+}$was successfully prepared.

1.6. Mercury detection with the cells-alginate hydrogel-based paper

The detection performance of cells-alginate hydrogel-based paper was tested by both laboratory water samples and industrial wastewater samples. The laboratory water samples were prepared by adding the standard solutions of metal ions into high purity deionized water. The industrial wastewater samples were prepared by adding the standard solutions of metal ions into industrial wastewater after being high speed centrifugation. Then, 30 μL of the aforementioned water samples were dripping on each center of cells-alginate hydrogel particles on the black paper strips. Then, the strip of cells-alginate hydrogel-based paper was placed into a dark chamber ultraviolet analyzer (ZF-20D, Shanghai Baoshangu Village Dianguang Instrument Factory). After incubation at room temperature for 5 min, it was taken a picture by a 16-million-pixel smartphone under the 365 nm ultraviolet lamp in the dark chamber ultraviolet analyzer. Finally, the ImageJ software was used to quantify the intensity of whole sensing area captured for each cells-alginate hydrogel particles on the picture. The intensity values calculated by the ImageJ software were used as the data to analyze.

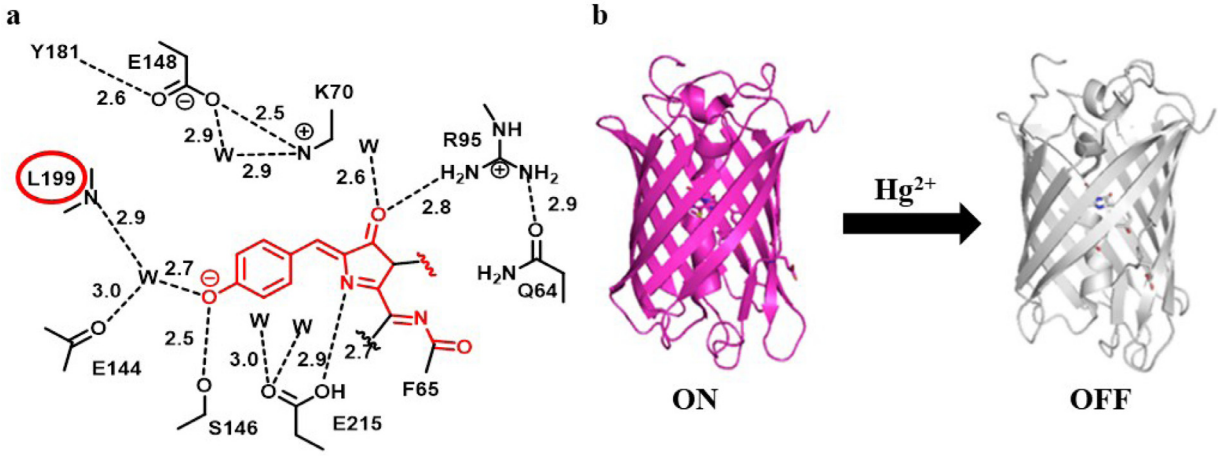

Fig. 1 – Engineering of a mercury binding site in close proximity to the chromophore of mCherry protein. (a) Schematic diagram of chromophore environment of mCherry protein. (b) Proposed schematic representation of fluorescence "turn-off" mechanism of the designed mCherry variant towards Hg^{2+}.

2. Results and discussion

2.1. *Designing of mercury-responsive fluorescent biosensor*

The fluorescent protein mCherry was obtained based on red fluorescent protein (RFP) by mutating the sites near the chromophore (Bevis and Glick, 2002; Campbell et al., 2002). In comparison to the progenitor, the second-generation monomeric red fluorescent protein mCherry has improved brightness and photostability (Shu et al., 2006). Similar to green fluorescent protein (GFP), its basic structure presents a cylindrical barrel shape with the chromophore surrounded by 11 β-sheet chains. In the presence of molecular oxygen, the Gln66-Tyr67-Gly68 peptide autocatalyzes and forms a chromophore through covalent bonds, which can be excited by light to produce fluorescence (Campbell et al., 2002; Shu et al., 2006; Yarbrough et al., 2001). Previous studies have shown that a number of selectively placed mutations around the chromophore resulting in specific fluorescence changes, thus demonstrating the protein's potential for the development of a biosensor (Jiang et al., 2015; Nadarajan et al., 2014; Ravikumar et al., 2016, 2015). In this study, we have focused on engineering a metal binding site in close proximity to the chromophore of mCherry protein. A series of mutations were designed by replacing the residues around the chromophore or involved in the hydrogen bond network nearby it with cysteines (Fig. 1a). Engineering cysteine residue in this region may help in the development of efficient mercury binding and enable a fluorescence turn-off mechanism in the presence of Hg^{2+} (Fig. 1b).

2.2. *Screening of mercury-responsive fluorescent biosensor by cell surface display technique*

In order to screen the mercury-responsive fluorescent biosensor in a simple way, the designed mutants of mCherry protein were expressed through fusing with membrane protein OmpA to decorate on outer-membrane of *E.coli* cells. Take mCherry L199C for example, as shown in Fig. 2a, the expression of fusion protein OmpA-mCherry L199C increased visibly after being induced near the theoretical value (calculated MW = 47.55 kDa) on the SDS-PAGE gel, and almost all of the fusion protein was obtained from the membrane fraction (Fig. 2b). According to previous researches (Wei et al., 2014, 2012), through fusing with outer-membrane protein OmpA, the fluorescent protein mCherry L199C was most likely displayed on the *E.coli* cell surface successfully. With expressing on the cell surface, the mutants of fluorescent protein mCherry can access to Hg^{2+} in the external environment di-

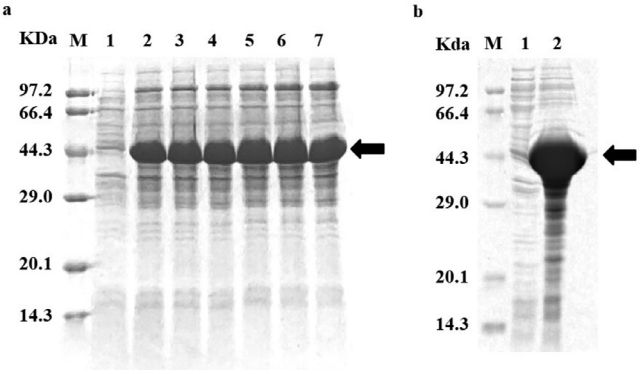

Fig. 2 – SDS-PAGE analysis of the fusion expression of mCherry L199C with OmpA protein. (a) The identification of being induced expression of fusion protein OmpA-mCherry L199C by 0.1 mmol/L IPTG on 14% SDS-PAGE (lane 1–7: 0, 1, 2, 3, 4, 6 and 8 h). (b) The membrane and cytoplasmic fractions of fusion protein OmpA-mCherry L199C identified on 14% SDS-PAGE (lane 1: cytoplasmic fraction, lane 2: membrane fraction). The black arrows in all the figures indicated the target proteins.

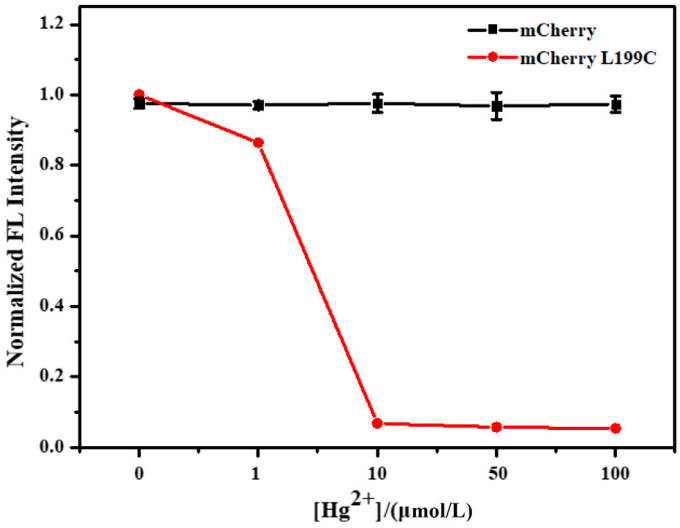

Fig. 3 – Change in fluorescence intensity of cells expressing wild type mCherry and mCherry L199C treated with different concentrations of Hg^{2+} (0–100 μmol/L). All the data are the means of five independent experiments. Error bars correspond to the standard deviations.

rectly. Therefore, simple and effective screening can be performed by the *E.coli* cells expressing mCherry mutants on the outer-membrane. By using the cell surface display technique, complicated and time-consuming procedures were avoided for purifying the variants of mCherry protein.

The screening results showed that the mutant mCherry L199C has a response to the stimulation of Hg^{2+}. As shown in Fig. 3, the cells expressing mutant mCherry L199C on the outer-membrane displayed strong intrinsic fluorescence. The fluorescence was decreased slightly in the presence of 1 μmol/L Hg^{2+}, and it was completely quenched when the concentration of Hg^{2+} increased to 10 μmol/L. In contrast, the fluorescence of the cells expressing wild type mCherry on the outer-membrane did not change significantly even the concentration of Hg^{2+}increased to 100 μmol/L. These significant differences could also be directly observed with the naked eye (Appendix A Fig. S4). The comparative experiments stated that the mutant mCherry L199C, which makes a response to Hg^{2+} stimulation, has great potential to be developed as a fluorescent biosensor for the detection of mercury pollution.

2.3. *Characterization of screened mercury-responsive fluorescent biosensor*

As above-demonstrated, the screened fluorescent biosensor (mCherry L199C) showed a drastic "turn-off" effect on the fluorescence intensity upon increasing the concentration of Hg^{2+}. The attenuation of fluorescence towards Hg^{2+} was further characterized in the concentration range of 1 ~ 10 μmol/L. As shown in the response curve (Fig. 4a), the fluorescence of cells expressing mCherry L199C on the outer-membrane showed progressively increased attenuation towards Hg^{2+}, and the degree of attenuation reached maximum at the concentration of 10 μmol/L. However, when treated by same concentration of other metal ions, cells expressing mCherry L199C on the outer-membrane did not have obvious attenuation in fluorescence intensity. These metal ions include transition-metal ions (Fe^{3+}, Ag^{+}, Cu^{2+}, Ni^{2+}, Zn^{2+}, Cd^{2+}, and Cr^{3+}) and the common heavy-metal contaminant Pb^{2+} (Fig. 4b). These results indicated the screened fluorescent biosensor mCherry L199C had good selectivity in detecting the heavy-metal contaminant Hg^{2+}.

In actual industrial production, the mercury pollution is always discharged along with other metal ions and into the water environment having different pH values. Thus, the performances of the fluorescent biosensor mCherry L199C towards Hg^{2+} were also evaluated in the presence of other metal ions and different pH environment. As shown in Fig. 4c and Fig. 4d, the response signals of cells expressing mCherry L199C on the outer-membrane towards Hg^{2+} were not greatly interfered by the aforementioned metal ions as well as the varying pH values (pH 4.0 ~ 10.0). These characterizations made the screened fluorescent biosensor mCherry L199C, which was expressed on the outer-membrane of *E.coli* cells, was practically feasible for on-site assessment of Hg^{2+} contamination.

2.4. *Preparation and stability characterization of the cells-alginate hydrogel-based paper*

For high-throughput fabrication and detection, the cells with mCherry L199C expressed on the outer-membrane were immobilized by the alginate hydrogel to develop the cells-alginate hydrogel-based paper. Further, an operation-simple and cost-effective method for mercury pollution detection was developed in combination with a smartphone and ImageJ software as the fluorescence intensity quantification devices. The operation procedure was present by the schematic diagram shown in Fig. 5a. By using these devices, the fluorescent stability and active stability were characterized for the prepared cells-alginate hydrogel-based paper. As shown in Fig. 5b and Fig. 5c, by storing at 4 °C in 0.1 mol/L $CaCl_2$ solution, the fluorescence intensity of cells-alginate hydrogel-

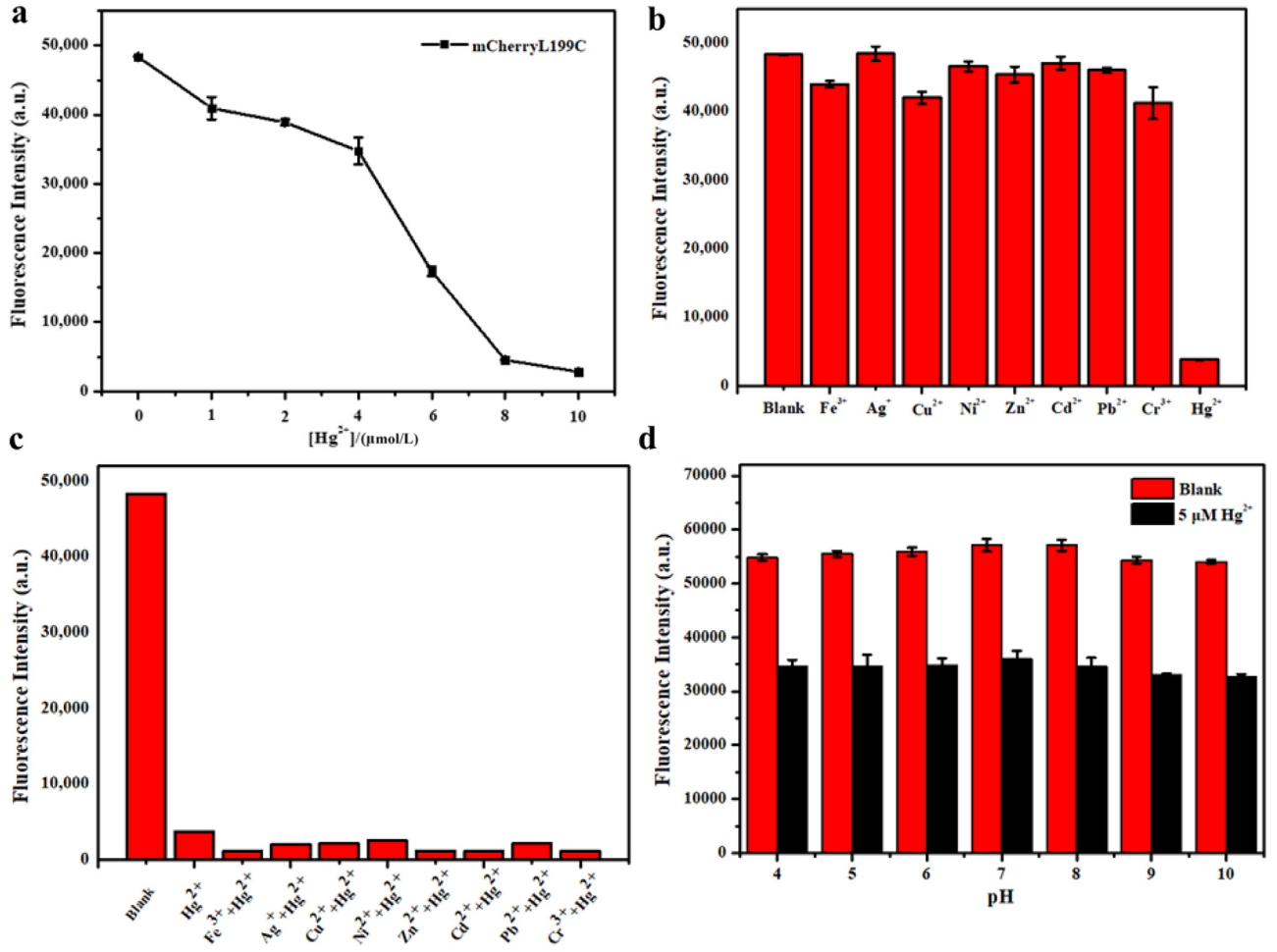

Fig. 4 – Properties characterization of mercury-responsive fluorescent biosensor mCherry L199C. (a) Change in fluorescence intensity of cells expressing mCherry L199C towards different concentrations of Hg^{2+} (0, 1, 2, 3, 4, 5, 6, 7, 8, 9, 10 μmol/L). (b) Change in fluorescence intensity of cells expressing mCherry L199C towards different metal ions (Fe^{3+}, Ag^{+}, Cu^{2+}, Ni^{2+}, Zn^{2+}, Cd^{2+}, Pb^{2+}, and Cr^{3+}) at the concentration of 10 μmol/L. (c) Change in fluorescence intensity of cells expressing mCherry L199C towards 10 μmol/L Hg^{2+} in the presence of competing metal ions (Fe^{3+}, Ag^{+}, Cu^{2+}, Ni^{2+}, Zn^{2+}, Cd^{2+}, Pb^{2+}, and Cr^{3+}) at the concentration of 10 μmol/L. (d) Change in fluorescence intensity of cells expressing mCherry L199C towards Hg^{2+} in different pH environment. All the data are the means of five independent experiments. Error bars correspond to the standard deviations.

based paper did not change significantly within 24 hr. More importantly, the cells-alginate hydrogel-based paper still kept good activity in the detection of Hg^{2+} after preserving for 24 hr, and the quenched fluorescence intensity remained unchanged in 60 min. These results indicated that the cells-alginate hydrogel-based paper can maintain a stable state for a certain period of time, which offer convenience in preserving and enough time for the observation of testing results.

2.5. *Detection of mercury with the cells-alginate hydrogel-based paper*

By using the cells-alginate hydrogel-based paper, micromole level of mercury ions in the high purity deionized water could be well detected in 5 min (Fig. 6a). In the range of 1 ~ 10 μmol/L, the intensity values calculated by the ImageJ software were sequentially reduced. There was no obvious linear relationship between the intensity and the concentration. When the concentration of Hg^{2+}exceeds 10 μmol/L, the intensity value no longer changed. The cells-alginate hydrogel-based paper still had good selectivity and strong anti-interference ability in the detection of Hg^{2+} (Fig. 6b and Fig. 6c). It could distinguish various metal ions from Hg^{2+} and resist the interferences of other metal ions. These metal ions not only include the transition-metal ions (Fe^{3+}, Ag^{+}, Cu^{2+}, Ni^{2+}, Zn^{2+}, Cd^{2+}, and Cr^{3+}) and heavy-metal ion Pb^{2+}, but also contain the alkaline ion Ca^{2+} used in the preparing of alginate hydrogel.

By determining the standard solution, a “marker” was developed for the cells-alginate hydrogel-based paper on the re-

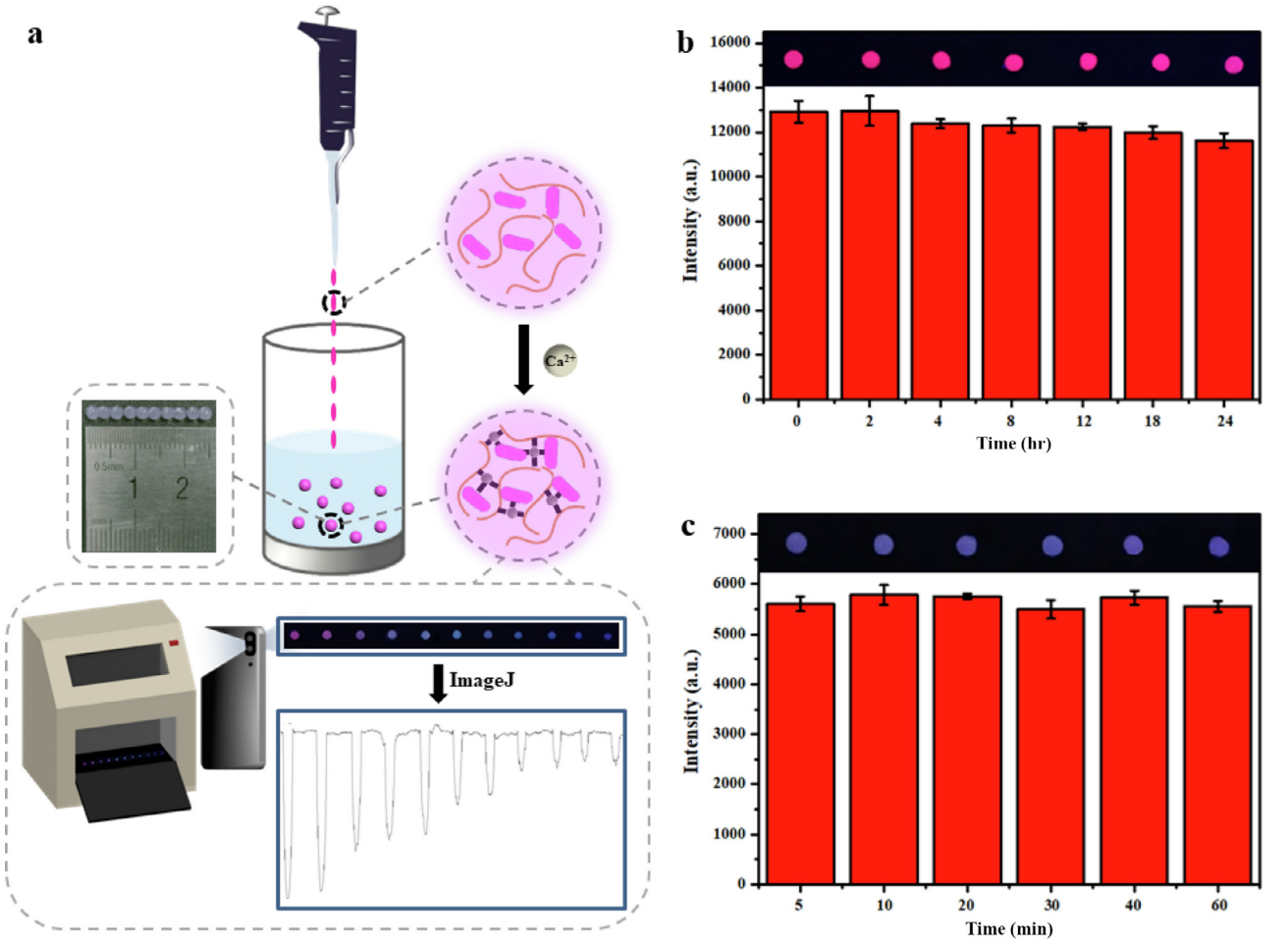

Fig. 5 – Preparation and stability characterization of the cells-alginate hydrogel-based paper. (a) Schematic diagram of the preparation of cells-alginate hydrogel-based paper and mercury detection with it by using a smartphone and ImageJ software as the fluorescence intensity quantification devices. (b) The color image captured by smart phone and corresponding intensity value quantified by ImageJ software of the cells-alginate hydrogel-based paper stored at 4 °C in 0.1 mol/L $CaCl_2$ solution for different time. (c) The color image captured by smart phone and corresponding intensity value quantified by ImageJ software of the cells-alginate hydrogel-based paper after being treated by 5 μmol/L Hg^{2+}. In (b) and (c), the intensity values quantified by ImageJ software are the means of five independent experiments. Error bars correspond to standard deviation.

lationship between the concentration of $Hg^{2+}$and the corresponding measured intensity value (Appendix A Fig. S5). The "marker" could be used to evaluate the content of Hg^{2+} in unknown samples. In the range of 1 ~ 10 μmol/L, the concentration of Hg^{2+} could be directly read according to the "marker". When the concentration of Hg^{2+} exceeds 10 μmol/L, the measured intensity value was close to the minimum intensity value in the "marker". Then, continuous dilution of the original solution was made until the measured intensity value fell between the maximum and the minimum of intensity value. By using this strategy, semi-quantitative results were offered by using the cells-alginate hydrogel-based paper to determine the contents of Hg^{2+} in industrial wastewater samples (Table 1). These could provide information about the range of mercury ion concentrations in water samples. Although the sensitivity is limited, it is already enough to preliminarily evaluate the industrial wastewater seriously polluted by mercury. Generally, the concentration of mercury contaminant in industrial wastewater is always more than micrograms per liter (equal to 5 μmol/L). For example, as the major source of mercury pollution, the chloralkali factory effluents contain mercury at the concentration of 15–50 μmol/L (Wagner-Döbler et al., 2000).

In comparison with other mercury detection methods, including the traditional techniques (such as AAS, AFS, and ICP-AES) and other previously developed mercury sensors, the present method for mercury detection have advantages on several aspects (Table 2). Firstly, the present method has no requirements for highly specialized facilities, laboratory workplaces, and professional operators. The identification devices

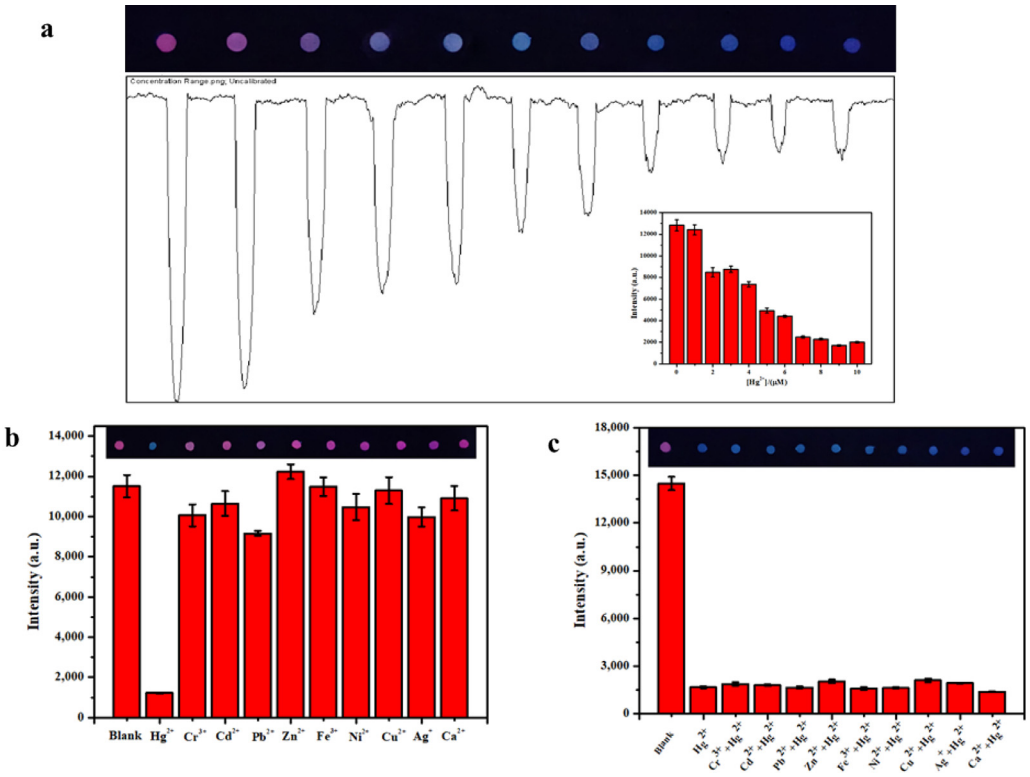

Fig. 6 – Detection of mercury with the cells-alginate hydrogel-based paper. (a) The color image captured by smart phone and corresponding intensity value quantified by ImageJ software of the cells-alginate hydrogel-based paper treated with different concentrations of Hg^{2+} (0, 1, 2, 3, 4, 5, 6, 7, 8, 9 and 10 μmol/L). (b) The color image captured by smart phone and corresponding intensity value quantified by ImageJ software of the cells-alginate hydrogel-based paper treated with different metal ions (Cr^{3+}, Cd^{2+}, Pb^{2+}, Zn^{2+}, Fe^{3+}, Ni^{2+}, Cu^{2+}, Ag^{+} and Ca^{2+}) at the concentration of 10 μmol/L. (c) The color image captured by smart phone and corresponding intensity value quantified by ImageJ software of the cells-alginate hydrogel-based paper treated with 10 μmol/L Hg^{2+} in the presence of competing metal ions (Cr^{3+}, Cd^{2+}, Pb^{2+}, Zn^{2+}, Fe^{3+}, Ni^{2+}, Cu^{2+}, Ag^{+} and Ca^{2+}) at the concentration of 10 μmol/L. The intensity values quantified by ImageJ software are the means of five independent experiments. Error bars correspond to standard deviation.

Table 1 – Evaluation of Hg^{2+} pollution in industrial wastewater samples by cells-alginate hydrogel-based paper.

Sample	Add (μmol/L)	Method of reading data	Found (μmol/L)
Industrial wastewater 1	4	Direct reading	4–5
	6	Direct reading	5–6
	8	Direct reading	7–8
	50	Reading after dilution	48–54
Industrial wastewater 2	4	Direct reading	4–5
	6	Direct reading	5–6
	8	Direct reading	7–8
	50	Reading after dilution	48–54

in this method are pervasive and commonplace, and they are convenient in carrying and operating. Secondly, the process of detection is easy and time-saving, which make it suitable for high throughput screening. All these advantages make this detection method suitable for rapid field testing of wastewater seriously polluted by mercury. However, the detection limit of this method needs further improvement for wider applications.

Table 2 – Comparison between different mercury detection methods and the present method.

Methods	Equipment	Workplace	Operator	Process	Detection time (HTS)	Detection limit (μmol/L)	Reference
AAS	Large instrument	Laboratory	Professional	Complicated	Time consuming	1.5×10^{-4}	(Giakisikli et al., 2013)
ICP-AES	Large instrument	Laboratory	Professional	Complicated	Time consuming	0.01	(Rudner et al., 1993)
ICP-MS	Large instrument	Laboratory	Professional	Complicated	Time consuming	1.25×10^{-4}	(Voica et al., 2009)
QDs	Spectrometer	Laboratory	Laypeople	Complicated	Rapid	0.008	(Yang et al., 2013)
Electrochemistry	Electrochemical workstation	Laboratory	Professional	Complicated	Time consuming	0.001	(Martín-Yerga et al., 2012)
Nanoparticle	Spectrometer	Laboratory	Laypeople	Complicated	Rapid	0.6	(Guo et al., 2015)
Cells-alginate hydrogel-based paper	Ultraviolet analyzer	Field testing	Laypeople	Simple	Rapid	1	This work

*HTS: High Throughput Screening.

3. Conclusion and implications

The fluorescent proteins have great potential for metal ions' detection through rational modification of the chromophore environment. In this research, the Hg^{2+}-sensing fluorescent biosensor mCherry L199C was successfully designed by introducing a cysteine in close proximity to the chromophore of mCherry protein. For rapid field testing of mercury pollution, the low-cost, lightweight, and disposable cells-alginate hydrogel-based paper was prepared by encapsulating the cells expressing mCherry L199C on the cell surface with alginate hydrogel. Then, simple procedure for mercury detection was developed by using the cells-alginate hydrogel-based paper combined with a smartphone and ImageJ software as the fluorescence intensity quantification devices. In this strategy, more fluorescent biosensors can be designed and applied for various metal ions' detection in an easy, fast, and economic manner. On the other hand, due to the genetically encodable, the developed fluorescent biosensors have great potential to be used as the tools for tracking metal dynamics inside living cells.

Acknowledgements

This work was supported by the Natural Science Foundation of Guangxi Province (No. 2018JJB120049), National Natural Science Foundation of China (No. 31800631), and the BAGUI Scholar Program of Guangxi Province of China.

Appendix A Supplementary data

Supplementary material associated with this article can be found, in the online version, at doi:10.1016/j.jes.2021.01.003.

REFERENCES

Ayyadurai, N., Saravanan Prabhu, N., Deepankumar, K., Lee, S.G., Jeong, H.H., Lee, C.S., et al., 2011. Development of a selective, sensitive, and reversible biosensor by the genetic incorporation of a metal-binding site into green fluorescent protein. Angew. Chem. Int. Ed. 50 (29), 6534–6537.

Bevis, B.J., Glick, B.S., 2002. Rapidly maturing variants of the Discosoma red fluorescent protein (DsRed). Nat. Biotechnol. 20 (1), 83–87.

Bridges, C.C., Zalups, R.K., 2017. Mechanisms involved in the transport of mercuric ions in target tissues. Arch. Toxicol. 91 (1), 63–81.

Campbell, R.E., Tour, O., Palmer, A.E., Steinbach, P.A., Baird, G.S., Zacharias, D.A., et al., 2002. A monomeric red fluorescent protein. Proc. Natl. Acad. Sci. USA. 99 (12), 7877–7882.

Chen, G., Guo, Z., Zeng, G., Tang, L., 2015. Fluorescent and colorimetric sensors for environmental mercury detection. Analyst 140 (16), 5400–5443.

Ekinci, M., Ceylan, E., Keleş, S., Cağatay, H.H., Apil, A., Tanyıldız, B., et al., 2014. Toxic effects of chronic mercury exposure on the retinal nerve fiber layer and macular and choroidal thickness in industrial mercury battery workers. Med. Sci. Monit. 20, 1284–1290.

Ellingsen, D.G., Efskind, J., Haug, E., Thomassen, Y., Martinsen, I., Gaarder, P.I., 2000. Effects of low mercury vapour exposure on the thyroid function in chloralkali workers. J. Appl. Toxicol. 20 (6), 483–489.

Gao, Y., Shi, Z., Long, Z., Wu, P., Zheng, C., Hou, X., 2012. Determination and speciation of mercury in environmental and biological samples by analytical atomic spectrometry. Microchem. J. 103, 1–14.

Giakisikli, G., Miró, M., Anthemidis, A., 2013. Integrated lab-in-syringe platform incorporating a membraneless gas–liquid separator for automatic cold vapor atomic absorption spectrometry. Anal. Chem. 85 (19), 8968–8972.

Guo, Y., Zhang, L., Zhang, S., Yang, Y., Chen, X., Zhang, M., 2015. Fluorescent carbon nanoparticles for the fluorescent detection of metal ions. Biosens. Bioelectron. 63, 61–71.

Hao, Z., Zhu, R., Chen, P.R., 2018. Genetically encoded fluorescent sensors for measuring transition and heavy metals in biological systems. Curr. Opin. Chem. Biol. 43, 87–96.
Jiang, T., Guo, D., Wang, Q., Wu, X., Li, Z., Zheng, Z., et al., 2015. Developing a genetically encoded green fluorescent protein mutant for sensitive light-up fluorescent sensing and cellular imaging of Hg(II). Anal. Chim. Acta. 876, 77–82.
Li, J., Zhu, J., Xu, K., 2014. Fluorescent metal nanoclusters: from synthesis to applications. Trends. Anal. Chem. 58, 90–98.
Liang, L.-.N., Jiang, G.-.B., Liu, J.-.F., Hu, J.-.T., 2003. Speciation analysis of mercury in seafood by using high-performance liquid chromatography on-line coupled with cold-vapor atomic fluorescence spectrometry via a post column microwave digestion. Anal. Chim. Acta. 477 (1), 131–137.
Liu, J., Karpus, J., Wegner, S.V., Chen, P.R., He, C., 2013. Genetically encoded copper(I) reporters with improved response for use in imaging. J. Am. Chem. Soc. 135 (8), 3144–3149.
Martín-Yerga, D., González-García, M.B., Costa-García, A., 2012. Use of nanohybrid materials as electrochemical transducers for mercury sensors. Sensor. Actuat. B-Chem. 165 (1), 143–150.
Mojammal, A.H.M., Back, S.K., Seo, Y.C., Kim, J.H., 2019. Mass balance and behavior of mercury in oil refinery facilities. Atmos. Pollut. Res. 10 (1), 145–151.
Nadarajan, S.P., Ravikumar, Y., Deepankumar, K., Lee, C.S., Yun, H., 2014. Engineering lead-sensing GFP through rational designing. Chem. Commun. 50 (100), 15979–15982.
Newman, R.H., Fosbrink, M.D., Zhang, J., 2011. Genetically encodable fluorescent biosensors for tracking signaling dynamics in living cells. Chem. Rev. 111 (5), 3614–3666.
Nolan, E.M., Lippard, S.J., 2008. Tools and tactics for the optical detection of mercuric ion. Chem. Rev. 108 (9), 3443–3480.
Özyurt, C., Üstükarcı, H., Evran, S., Telefoncu, A., 2019. MerR-fluorescent protein chimera biosensor for fast and sensitive detection of Hg^{2+} in drinking water. Appl. Biochem. 66 (5), 731–737.
Qin, Y., Sammond, D.W., Braselmann, E., Carpenter, M.C., Palmer, A.E., 2016. Development of an optical Zn^{2+} probe based on a single fluorescent protein. ACS. Chem. Biol. 11 (10), 2744–2751.
Ravikumar, Y., Nadarajan, S.P., Lee, C.S., Jung, S., Bae, D.H., Yun, H., 2016. FMN-based fluorescent proteins as heavy metal sensors against mercury ions. J. Microbiol. Biotechnol. 26 (3), 530–539.
Ravikumar, Y., Nadarajan, S.P., Lee, C.S., Rhee, J.K., Yun, H., 2015. A new-generation fluorescent-based metal sensor - iLOV protein. J. Microbiol. Biotechnol. 25 (4), 503–510.
Rudner, P.C., de Torres, A.G., Pavón, J.M.C., 1993. On-line preconcentration and determination of mercury by flow injection inductively coupled plasma atomic emission spectrometry. J. Anal. Atom. Spectrom. 8 (5), 705–709.
Sánchez-Rodas, D., Corns, W.T., Chen, B., Stockwell, P.B., 2010. Atomic Fluorescence Spectrometry: a suitable detection technique in speciation studies for arsenic, selenium, antimony and mercury. J. Anal. At. Spectrom. 25 (7), 933–946.
Semu, E., Singh, B.R., Selmer-Olsen, A.R., 1986. Mercury pollution of effluent, air, and soil near a battery factory in Tanzania. Water. Air. Soil. Pollut. 27 (1), 141–146.
Shu, X., Shaner, N.C., Yarbrough, C.A., Tsien, R.Y., Remington, S.J., 2006. Novel chromophores and buried charges control color in mFruits. Biochemistry 45 (32), 9639–9647.
Syversen, T., Kaur, P., 2012. The toxicology of mercury and its compounds. J. Trace. Elem. Med. Bio. 26 (4), 215–226.
Tchounwou, P.B., Ayensu, W.K., Ninashvili, N., Sutton, D., 2003. Review: environmental exposure to mercury and its toxicopathologic implications for public health. Environ. Toxicol. 18 (3), 149–175.
van Bloois, E., Winter, R.T., Kolmar, H., Fraaije, M.W., 2011. Decorating microbes: surface display of proteins on *Escherichia coli*. Trends. Biotechnol. 29 (2), 79–86.
Voica, C., Dehelean, A., Pamula, A., 2009. Method validation for determination of heavy metals in wine and slightly alcoholic beverages by ICP-MS. J. Phys. Conf. Ser. 182, 012036.
Wagner-Döbler, I., Canstein, H., Li, Y., Timmis, K., Deckwer, W.D., 2000. Removal of mercury from chemical wastewater by microoganisms in technical scale. Environ. Sci. Technol. 34.
Wang, Q., Kim, D., Dionysiou, D.D., Sorial, G.A., Timberlake, D., 2004. Sources and remediation for mercury contamination in aquatic systems—a literature review. Environ. Pollut. 131 (2), 323–336.
Wei, W., Liu, X., Sun, P., Wang, X., Zhu, H., Hong, M., et al., 2014. Simple whole-cell biodetection and bioremediation of heavy metals based on an engineered lead-specific operon. Environ. Sci. Technol. 48 (6), 3363–3371.
Wei, W., Zhu, T., Wang, Y., Yang, H., Hao, Z., Chen, P.R., et al., 2012. Engineering a gold-specific regulon for cell-based visual detection and recovery of gold. Chem. Sci. 3 (6), 1780–1784.
Yang, T., He, Q., Liu, Y., Zhu, C., Zhao, D., 2013. Water-soluble *N*-Acetyl-L-cysteine-Capped CdTe quantum dots application for Hg(II) detection. J. Anal. Methods. Chem. 2013, 902951.
Yarbrough, D., Wachter, R.M., Kallio, K., Matz, M.V., Remington, S.J., 2001. Refined crystal structure of DsRed, a red fluorescent protein from coral, at 2.0-Å resolution. Proc. Natl. Acad. Sci. USA. 98 (2), 462–467.
Zhang, J., Cheng, F., Li, J., Zhu, J., Lu, Y., 2016. Fluorescent nanoprobes for sensing and imaging of metal ions: recent advances and future perspectives. Nano. Today. 11 (3), 309–329.